LIMNOLOGY and OCEANOGRAPHY



© 2024 The Authors. *Limnology and Oceanography* published by Wiley Periodicals LLC on behalf of Association for the Sciences of Limnology and Oceanography. doi: 10.1002/lno.12536

Vertical trophic structure and niche partitioning of gelatinous predators in a pelagic food web: Insights from stable isotopes of siphonophores

Elizabeth D. Hetherington ⁰, ^{1*} Hilary G. Close ⁰, ² Steven H. D. Haddock, ³ Alejandro Damian-Serrano ⁰, ^{4,5} Casey W. Dunn ⁰, ⁴ Natalie J. Wallsgrove, ⁶ Shannon C. Doherty, ^{2,7} C. Anela Choy ⁰ 1*

¹Integrative Oceanography Division, Scripps Institution of Oceanography, University of California San Diego, La Jolla, California, USA

Abstract

Gelatinous zooplankton are increasingly recognized as key components of pelagic ecosystems, and there have been many recent insights into their ecology and roles in food webs. To examine the trophic ecology of siphonophores (Cnidaria, Hydrozoa), we used bulk (carbon and nitrogen) and compound-specific (nitrogen) isotope analysis of individual amino acids (CSIA-AA). We collected samples of 15 siphonophore genera using blue-water diving, midwater trawls, and remotely operated vehicles in the California Current Ecosystem, from 0 to 3000 m. We examined the basal resources supporting siphonophore nutrition by comparing their isotope values to those of contemporaneously collected sinking and suspended particles (0-500 m). Stable isotope values provided novel insights into siphonophore trophic ecology, indicating considerable niche overlap between calycophoran and physonect siphonophores. However, there were clear relationships between siphonophore trophic positions and phylogeny, and the highest siphonophore trophic positions were restricted to physonects. Bulk and source amino acid nitrogen isotope (δ^{15} N) values of siphonophores and suspended particles all increased significantly with increasing collection depth. In contrast, siphonophore trophic positions did not increase with increasing collection depth. This suggests that microbially reworked, deep, suspended particles with higher δ^{15} N values than surface particles, likely indirectly support deep-pelagic siphonophores. Siphonophores feed upon a range of prey, from small crustaceans to fishes, and we show that their measured trophic positions reflect this trophic diversity, spanning 1.5 trophic levels (range 2.4–4.0). Further, we demonstrate that CSIA-AA can elucidate the feeding ecology of gelatinous zooplankton and distinguish between nutritional resources across vertical habitats. These findings improve our understanding of the functional roles of gelatinous zooplankton and energy flow through pelagic food webs.

This is an open access article under the terms of the Creative Commons Attribution License, which permits use, distribution and reproduction in any medium, provided the original work is properly cited.

Additional Supporting Information may be found in the online version of this article.

Author Contribution Statement: We confirm that each author has contributed to this manuscript: The manuscript concept was developed collaboratively between C.A.C. and E.D.H. E.D.H., S.H.D.H., A.D.S., A.L., and C.A.C. participated in field collections of siphonophores. N.J.W. and C.A.C. performed bulk and CSIA isotope analyses on siphonophores. H.G.C., C.A.C. and S.D. collected particle samples and H.G.C. and S.D. performed isotope analyses. E.D.H. led all data analyses and wrote the first draft of the manuscript. All authors contributed to the editing process and approved the manuscript's submission to *Limnology and Oceanography*.

Food web linkages between gelatinous animals remain a poorly resolved component of pelagic food webs and ecosystem models (Pauly et al. 2009; Lamb et al. 2019). Gelatinous zooplankton is a "catch-all" term that describes a diverse assemblage of animals with high (> 95%) water content that spans several phyla (Condon et al. 2012). They are also functionally diverse, serving various trophic roles as grazers, predators (Hays et al. 2018; Décima et al. 2019), and prey for higher trophic level species (Cardona et al. 2012; Hoving and Haddock 2017). Some gelatinous zooplankton (e.g., pelagic tunicates) undergo blooms, which can drastically alter community composition, biomass, and food web structure (Brodeur et al. 2019; Lyle et al. 2022). Identifying trophic relationships among gelatinous zooplankton is, therefore, essential for understanding how energy flows through ecosystems and

²University of Miami, Rosenstiel School of Marine, Atmospheric, and Earth Science, Miami, Florida, USA

³Monterey Bay Aquarium Research Institute, Moss Landing, California, USA

⁴Department of Ecology and Evolutionary Biology, Yale University, New Haven, Connecticut, USA

⁵University of Oregon, Institute of Ecology and Evolution, Eugene, Oregon, USA

⁶Department of Earth Sciences, University of Hawaii, Honolulu, Hawaii, USA

⁷University of Alaska Fairbanks, College of Fisheries and Ocean Sciences, Fairbanks, Alaska, USA

^{*}Correspondence: ehetheri@ucsd.edu; anela@ucsd.edu

for predicting how food webs will respond to environmental and anthropogenic pressures.

Certain gelatinous zooplankton are particularly fragile and difficult to collect with common shipboard sampling techniques. Siphonophores (Cnidaria, Hydrozoa) are often disaggregated, destroyed, or undersampled with trawls (Remsen et al. 2004; Hetherington et al. 2022a), but they are ubiquitous in marine systems (Robison et al. 1998; Condon et al. 2012; Lucas et al. 2014). Siphonophores are present across the water column, and their unique biology likely allows them to occupy numerous trophic niches in pelagic food webs (Damian-Serrano et al. 2021a,b). Siphonophores are colonial animals made of multiple types of specialized zooids, with tentacles that often bear complex side branches (tentilla) with stinging nematocysts (Fig. 1; Mapstone 2014). These tentacles are generally carried by gastrozooids that are specialized for and exclusively used in feeding. Unlike many metazoans that have one mouth on one end of the body for feeding, siphonophores can have hundreds of gastrozooids that can

feed independently along the length of the colony. Tentillum morphology is highly diverse (Damian-Serrano et al. 2021*b*) and related to high interspecific variation in diet and preytype specialization (Damian-Serrano et al. 2021*a*).

Seminal research on siphonophore predation relied on the visual analysis of the contents of gastrozooids from specimens that were collected via blue-water diving, which allows for the collection of intact, fragile colonies within diving depths in the upper ~ 30 m (Biggs 1977; Purcell 1981a). The very scarce available siphonophore-prey data from the deep pelagic indicate that siphonophores are central predators that are highly connected in pelagic food webs and feed on diverse taxa (Choy et al. 2017). Many siphonophores undergo daily vertical migrations, but the degree to which they may connect epi- and deep pelagic food webs is unknown. Siphonophore diet varies across species, and many species are likely specialists (e.g., *Rhizophysa* and *Erenna* are fish specialists) (Purcell 1981a; Haddock et al. 2005). Recent work suggests that deeppelagic siphonophores may be more specialized than

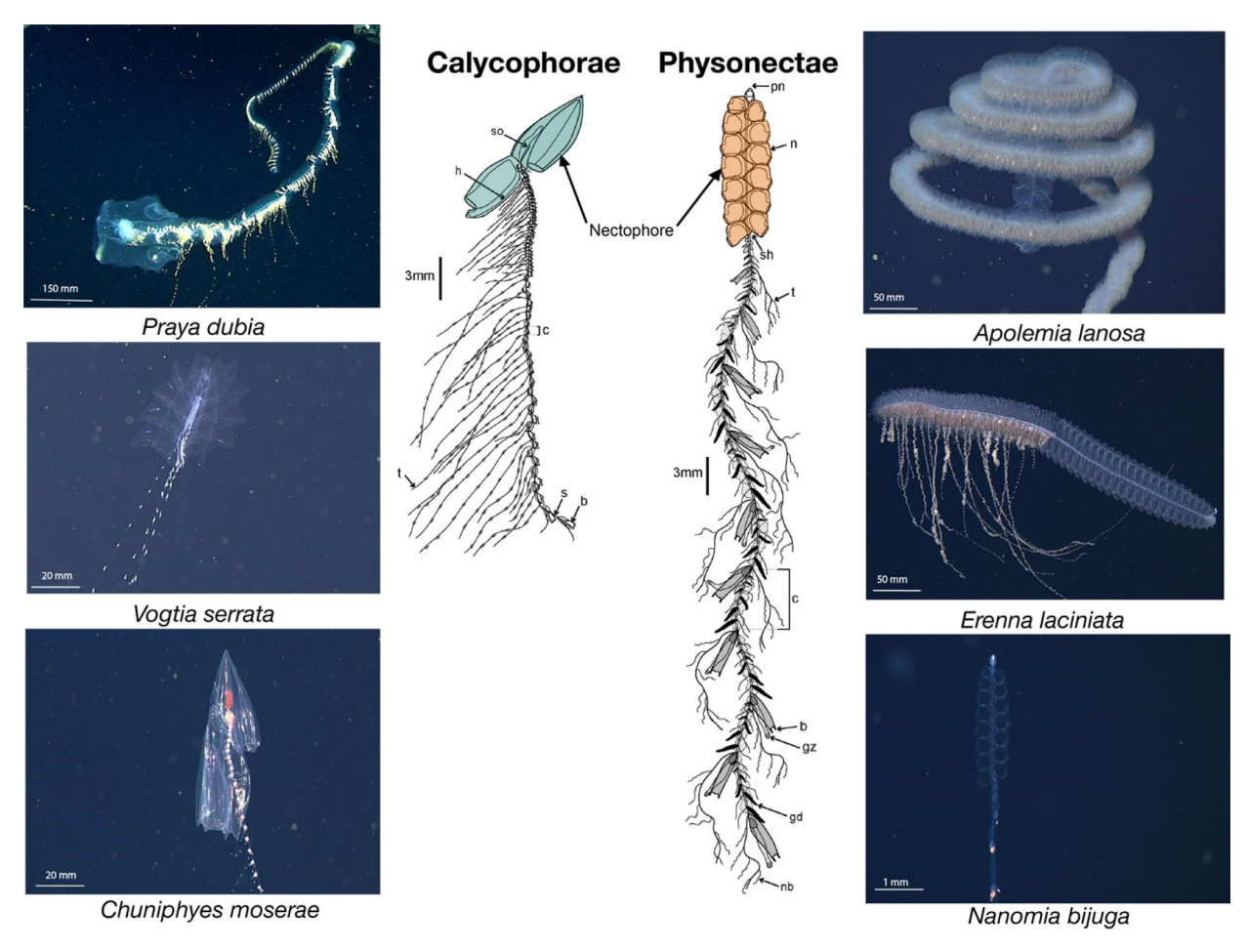


Fig. 1. Center: Illustrations of *Lensia conoidea* (Calycophorae) and *Nanomia bijuga* (Physonectae), edited from Mapstone (2014), where blue and orange shading highlight nectophores (swimming bells), which were primarily sampled for stable isotope analyses. Images from remotely operated vehicles show a subset of representative calycophoran (left) and physonect (right) species that were sampled for this study (Photo credits: Monterey Bay Aquarium Research Institute). Scale bars were estimated using nectophore lengths for each species, which were derived from the literature.

epipelagic species (Hetherington et al. 2022b), but few studies examine siphonophore trophic ecology across species and depth habitats within a food web. A recent DNA metabarcoding study of siphonophore gut contents (Damian-Serrano et al. 2022) identified prey in 24 siphonophore species across depth habitats, finding similar representations of small, hard-bodied, and large gelatinous prey in shallow- and deepdwelling species. Like visual observations, these analyses represent a dietary snapshot rather than a diet or trophic position integrated over time.

Biochemical tracers can aid in identifying trophic linkages in the jelly web because soft-bodied animals are generally poorly detected through visual gut contents analysis (Zeman et al. 2018; Milisenda et al. 2018; Chi et al. 2021). Stable isotope analysis of carbon and nitrogen are routinely used to examine the sources of primary production in an ecosystem and to infer the trophic positions of consumers (DeNiro and Epstein 1978, 1981; Fry 2006). Stable isotope analysis is particularly advantageous for siphonophores because it requires a tissue sample and not the collection of a fully intact colony. Stable isotope values can provide trophic position estimates and diet integrated over time (determined by tissue turnover rate), unlike dietary snapshots inferred from gut contents analysis (Purcell 1981a), gut content DNA metabarcoding (Damian-Serrano et al. 2022), or in situ feeding observations (Choy et al. 2017).

Stable nitrogen isotope ($\delta^{15}N$) values from bulk tissues $(\delta^{15}N_{Bulk})$ of consumers reflect both consumer diet and the δ15N value at the base of the food web (McClelland and Montoya 2002; Chikaraishi et al. 2009). Baseline δ^{15} N values are dependent on N-cycling biogeochemistry and can vary spatially (Graham et al. 2010), temporally (Rolff 2000; Kurle and McWhorter 2017), and vertically (Hannides et al. 2013). Compound-specific isotope analysis of amino acids (CSIA-AA) is a tool that constrains baseline variability and estimates consumer trophic position. CSIA-AA relies on the analysis of individual amino acids since certain "source" amino acids (e.g., phenylalanine) reflect the isotopic signature of the base of a food web, while other "trophic" acids (e.g., glutamic acid) reflect the consumer's diet (McClelland and Montoya 2002; Chikaraishi et al. 2009). Source and trophic amino acids are used to estimate trophic position while accounting for baseline variability in δ^{15} N values (Popp et al. 2007; Chikaraishi et al. 2009). Source amino acid δ^{15} N values can also identify distinct basal resources supporting consumers (e.g., epipelagic vs. deep particulate organic matter) (Hannides et al. 2013; Gloeckler et al. 2018; Close 2019; Romero-Romero et al. 2020; Shea et al. 2023). Source amino acid $\delta^{15}N$ values of siphonophores and particles can, therefore, be used to link siphonophores to near-surface (defined here as < 50 m collection depth) vs. deeper (sinking and/or suspended particle) food webs.

We collected siphonophore colonies in the epi-, meso-, and bathypelagic in the California Current Ecosystem to examine

siphonophore trophic ecology and resource use. Using stable isotope values of siphonophores, we compared isotopic niche widths across suborders and species and estimated siphonophore trophic positions. We also collected three size classes of particles (representing suspended and sinking particle pools; Lam et al. 2011; Lam and Marchal 2015) to identify vertical gradients in δ^{15} N values and the corresponding siphonophore linkages to epipelagic organic matter vs. deep particles.

Methods

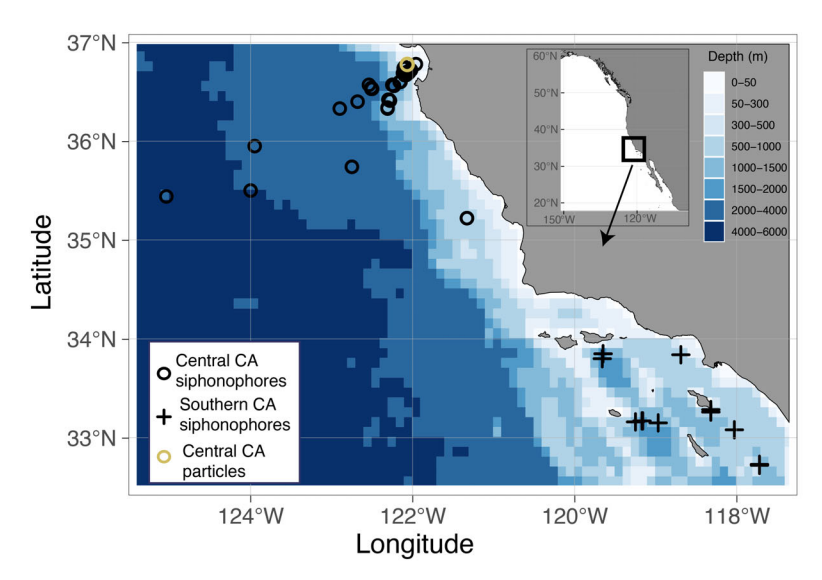
Sample collection and processing for stable isotope analyses

We collected samples on research cruises across multiple years (2014–2021) in Monterey Bay, California and the southern California Current Ecosystem (Fig. 2). To collect siphonophores, we used blue-water diving (0–25 m; Haddock and Heine 2005), the remotely operated vehicle *Doc Ricketts* (150–4000 m), and a midwater Tucker trawl (0–500 m). We collected siphonophore colonies representing at least 3 samples from 15 siphonophore genera (Table 1). Sample size varied among taxa. We collected smaller sample sizes for seven additional genera (*Kephyes, Muggiaea, Physophora, Desmophyes, Halistemma, Lensia,* and *Resomia*). Due to the limited sample size for those siphonophores, they were only included in analyses that compared bulk isotope values across suborders and depth habitats.

Collections included species for which published diet data or trophic position estimates are limited or do not exist (Table 1). We used siphonophore collection depths to examine vertical gradients in $\delta^{15}N$ values. All samples collected via blue-water diving were assigned a depth of 10 m, which was the average depth of collection dives. Discrete collection depths (to the nearest meter) were used for samples collected by remotely operated vehicles, and the midpoint depth of each trawl, based on the minimum and maximum depths, was used for samples from net tows. To ensure that siphonophore collection depths were representative of their typical depth habitat, we compared them to daytime depths recorded from historical remotely operated vehicle observations from the Monterey Bay Aquarium Research Institute's Video Annotation and Reference System (Schlining and Stout 2006) (Supporting Information Fig. SM1). This was only possible for a subset of species as remotely operated vehicle observations do not fully include epipelagic species that we sampled by blue-water diving.

Stable isotope analyses of siphonophores

To remove potential biases associated with tissue-specific variability in stable isotope values, we sampled the gelatinous swimming bells (nectophores; Fig. 1) of siphonophores. This approach was possible for most specimens, except for physonect species that are extremely fragile or have nectosomes that are a small fraction of the colony length and are often not collected.



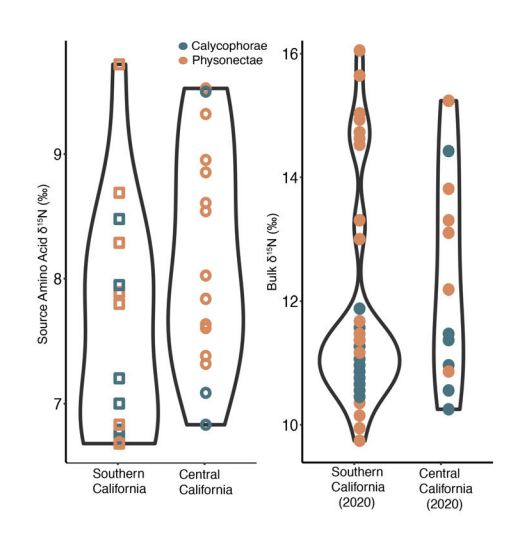


Fig. 2. (Left) Map of bathymetry and sample locations in the central and southern California Current from 2014 to 2021. Symbols indicate the sample locations where siphonophores (black) and particles (yellow) were collected for stable isotope analyses, where the shape corresponds to the sampling region. Particles were collected in 2017 (N = 28), siphonophores in southern CA were collected in 2020–2021 (N = 47), and siphonophores in central CA were collected in 2014–2021 (N = 155). (Right) There was no difference in source amino acid or bulk δ^{15} N values between sampling regions, where color denotes siphonophore suborder.

For these species (e.g., *Apolemia* spp.), we used the gelatinous bracts and pieces of the siphosome, excluding gastrozooids. For small individuals (*Diphyes dispar, Nanomia bijuga*, and *Sphaeronectes koellikeri*), we pooled nectophores from several colonies that were captured at the same time and sampling location to obtain an adequate mass for isotope analyses. We did not measure siphonophore length or weight. Since siphonophores are colonial, nectophore sizes are not predictive of overall colony size. A previous study found no relationship between isotope values and nectophore lengths (Chi et al. 2021).

Siphonophores were identified to the finest taxonomic level, which was either genus or species. For some genera, there are likely undescribed and/or cryptic species (e.g., *Apolemia*), and for these taxa, genus-level identifications were used. All siphonophores were rinsed with deionized water and frozen at -80° C until further processing. Siphonophore tissues were weighed, lyophilized, packaged into tin capsules for bulk isotope analysis, and analyzed at the University of Hawaii's Biogeochemical Stable Isotope Facility.

For bulk stable isotope analysis, 202 siphonophore samples were analyzed using a Costech elemental combustion system coupled to a Thermo-Finnigan Delta XP isotope ratio mass spectrometer (IRMS) via a Thermo Scientific Conflo IV. All stable isotope values are reported in permil (‰) vs. AIR and Vienna Pee Dee Belemnite for nitrogen and carbon, respectively. A subset of samples was selected for CSIA-AA (Table 1); for each of 10 siphonophore genera, we analyzed three to four samples. These specific taxa were selected as representatives of different depth habitats, suborders, and hypothesized diets (Table 1).

CSIA-AA was also conducted at the University of Hawaii's Biogeochemical Stable Isotope Facility using acid hydrolysis followed by derivatization (see Popp et al. 2007 and Hannides et al. 2013 for details). Derivatives were analyzed using a Thermo-Finnigan Delta V Plus IRMS, interfaced with a Thermo Trace GC gas chromatograph via GC-C III combustion furnace (980°C), reduction furnace (650°C), and a liquid nitrogen cold trap. Samples were injected (split/splitless injector, splitless mode) with a 180°C injector temperature and a constant helium flow rate of 1.4 mL min⁻¹. For quality control, we analyzed an amino acid suite, with known $\delta^{15}N$ values of 14 amino acids, every three to four sample injections. Internal reference compounds, L-2-aminoadipic acid and L-(+)-norleucine of known nitrogen isotopic composition, were co-injected with samples and suites and used as a measure of accuracy and instrument precision. Samples for CSIA-AA are typically analyzed in triplicate runs. Our samples, however, required six runs to obtain peaks for all amino acids due to the inordinate relative abundance of glycine compared to all other amino acids. It is unclear why glycine peaks were large, although we note that the relative abundances of the different amino acids can vary by taxa and tissue type. It is unknown whether this is common for siphonophores as no other published CSIA-AA studies currently exist.

Glycine peaks were so large that the chromatography surrounding glycine was deleteriously affected when injecting volumes large enough to detect all amino acids of interest. To overcome this, we analyzed samples in triplicate at injection volumes that allowed for good chromatography around glycine and then again in triplicate at a larger injection volume

Table 1. Siphonophore species, mean collection depth (\pm SDs when applicable), hypothesized diet, the number of samples analyzed for bulk stable isotope analysis (SIA) with the number of samples analyzed for CSIA-AA in parentheses, and bulk δ^{15} N and δ^{13} C values (\pm SD). The cluster column was determined by a Ward's hierarchical cluster analysis of bulk isotope values. Hypothesized diets were based on a limited number of previous studies that characterized siphonophore diets from remotely operated vehicle observations (Choy et al. 2017), gut contents analysis (Purcell 1981a,b), or metabarcoding of gut contents (Damian-Serrano et al. 2022).

| | _ | Collection | | Bulk SIA N | a15 | -13 - to t | |
|--------------|--------------------------|---------------|---|------------|------------------|-----------------------|---------|
| Suborder | Genus or species | depth (m) | Hypothesized diet | (CSIA N) | δ'3N (‰) | δ ¹³ C (‰) | Cluster |
| Calycophorae | Chuniphyes sp. | $760{\pm}693$ | Small crustaceans | 22 (4) | $11.3 {\pm} 1.2$ | $-20.2{\pm}1.3$ | 4 |
| | Diphyes dispar | 10 | Copepods, euphausiids, other small crustaceans, salps | 22 (3) | 11.0±0.3 | −19.5±0.3 | 3 |
| | Praya dubia | 261±146 | Gelatinous, krill, copepods | 6 (3) | 11.2±1.1 | $-20.8 {\pm} 0.8$ | 4 |
| | Sphaeronectes koellikeri | 10 | Copepods, decapods, small crustaceans | 5 | 9.8±1.6 | $-20.6 {\pm} 0.2$ | 4 |
| | Rosacea sp. | 10 | Copepods, mollusks, chaetognaths | 8 | $9.2{\pm}0.8$ | -21.1 ± 1.3 | 4 |
| | Vogtia serrata | $876{\pm}670$ | Ostracods | 3 | $12.1 {\pm} 0.4$ | $-19.8 {\pm} 0.3$ | 3 |
| Physonectae | Agalma elegans | 10 | No observations | 3 (3) | $10.1 {\pm} 0.6$ | $-20.3 {\pm} 0.5$ | |
| | Apolemia spp. | 722±257 | Gelatinous, fishes, crustaceans, chaetognaths | 37 (3) | 14.1±1.3 | $-20.3 {\pm} 0.9$ | 2 |
| | Bargmannia elongata | 773±632 | Large crustaceans, small crustaceans, cephalopods | 33 (4) | 13.0±1.2 | $-20.2 {\pm} 0.7$ | 2 |
| | Erenna spp. | 1752±512 | Fishes | 4 (3) | $14.4 {\pm} 1.3$ | $-21.4 {\pm} 0.7$ | 1 |
| | Forskalia spp. | 390±59 | Copepods, crustaceans | 4 | $11.3 {\pm} 0.8$ | $-21.1 {\pm} 0.6$ | 4 |
| | Frillagalma vityazi | $474{\pm}26$ | No observations | 4 | $11.7 {\pm} 0.5$ | $-20.7 {\pm} 0.7$ | 4 |
| | Lychnagalma utricularia | 364±97 | Large crustaceans, decapods, euphausiids | 7 (3) | 14.3±0.7 | -20.1 ± 0.5 | 2 |
| | Nanomia bijuga | 247±133 | Krill, copepods, small crustaceans | 30 (3) | 11.1 ± 0.8 | $-19.8{\pm}1.2$ | 3 |
| | Stephanomia amphytridis | 903±514 | Fishes | 3 (3) | $13.3{\pm}2.3$ | $-21.2 {\pm} 0.2$ | 1 |

to allow smaller amino acids to be detected while backflushing the large glycine peak out of the chromatogram. We obtained well-defined peaks for 14 amino acids, which were grouped into standard "trophic" and "source" categories based on previous studies (McClelland and Montoya 2002; Popp et al. 2007; Chikaraishi et al. 2009). Methionine and tyrosine were less frequently detected in 18 and 8 of the 33 samples, respectively. The average analytical uncertainty for the samples, across all amino acids, was 0.4% for $\delta^{15}N$ but ranged from 0.0% to 2.5%.

Stable isotope analyses of particles

We compared our siphonophore isotope data to contemporaneous analysis of particle biogeochemistry in Monterey Bay. Particles were collected on 31 July and 03 August 2017, using in situ filtration (WTS-LV; McLane Research Laboratories). Particles were collected at discrete depths from 0 to 500 m at the Midwater 1 mesopelagic time-series observation site in Monterey Bay, CA (36.78°N, 122.058°W; 1600 m total water depth). Filters were mounted on mini-MULVFS 3-tiered filter holders, which are designed to exclude swimming zooplankton but include all other particulate material (Bishop et al. 2012). The three size classes were collected using three

filters placed on sequential tiers: $100~\mu m$ nylon (Nitex) mesh with $150~\mu m$ nylon (Nitex) mesh backing, $20~\mu m$ nylon (Nitex) mesh backing, and two, stacked $0.7~\mu m$ pre-combusted glass microfiber filters (GF/F).

The particle size fractions were selected based on previous studies, which have set a precedent for using size fractions to represent separate sinking and suspended pools in particles collected via in situ filtration (Lam et al. 2011; Lam and Marchal 2015). Sinking particles have previously been represented by the large size fraction (typically > 53 μ m or > 70 μ m), while suspended particles were represented by the small size fraction (1–53 or 0.7–53 μ m; Lam et al. 2011; Lam and Marchal 2015). The particle size fractions presented here can be similarly defined as small/suspended (0.7–20 μ m) and large/sinking (> 100 μ m), with an intermediate size class (20–100 μ m).

Nitex mesh was pre-cleaned in 1.2 N hydrochloric acid and methanol; GF/Fs were pre-combusted at 450° C for 24 h. Filters were held on ice immediately after field collections and then transferred to combusted foil packets and stored at -80° C within approximately 3 h of initial collection. Large particles collected on Nitex were resuspended in 0.2- μ m filtered

seawater, re-filtered onto GF/Fs, freeze-dried, and checked for swimmers under microscopy as described by Doherty et al. (2021) and Wojtal et al. (2023); any detected swimmers were removed. All GF/Fs were freeze-dried and analyzed for bulk stable isotopes and CSIA-AA at the Marine Organic and Isotope Geochemistry Facility at the University of Miami following procedures modified by Hannides et al. (2013). All isotopic values (siphonophores and particles) and sample information are available through the Biological & Chemical Oceanography Data Management Office (BCO-DMO) (https://www.bco-dmo.org/project/738543).

Data analysis

Data analyses were conducted using the R programming language (RStudio Team 2020). Isotopic niche widths were estimated using the package "SIBER," Stable Isotope Bayesian Ellipses in R (Jackson et al. 2011). We first calculated the total Standard Ellipse Areas of siphonophores using bulk $\delta^{15}N$ $(\delta^{15}N_{Bulk})$ and $\delta^{13}C$ $(\delta^{13}C_{Bulk})$ values, corrected for sample size. We also used a Bayesian approach to infer Standard Ellipse Areas (Bayesian Standard Ellipse Areas) using Markov chain Monte Carlo (MCMC) simulations. Posterior estimates were based on a set of 10,000 iterative draws from MCMC simulations. For each draw, bivariate means and covariance matrix values were used to construct an ellipse and derive Bayesian Standard Ellipse Areas values. Using functions in SIBER, we compared Bayesian Standard Ellipse Areas between siphonophore suborders (Calycophorae and Physonectae) between collection depths (epi-, meso-, and bathypelagic).

We performed Ward's hierarchical cluster analysis on $\delta^{15}N_{Bulk}$ and $\delta^{13}C_{Bulk}$ values using the function "hclust" in R. We created a dissimilarity matrix using Euclidean distances and complete linkage. This method computes all pairwise dissimilarities between groups (clusters) and considers the largest dissimilarity as the distance between those groups. We assessed the strength of the clustering structure by calculating the agglomerative coefficient, which ranges from 0 to 1, where high values suggest robust separation between groups (i.e., strong clustering structure). In dendrograms, the height of the vertical axis fusion indicates the dissimilarity between observations, whereas higher heights indicate less similar observations.

The "step" function was used to perform forward–backward stepwise multiple regression to examine the relationships between $\delta^{15} N_{Bulk}$ and depth, latitude, longitude, year, and month. Akaike information criterion (AIC) values were used to determine the number of variables to include in the final model, where a reduction in AIC > 2 was used as a cutoff. χ^2 tests were used to determine whether the models were statistically different.

Amino acid $\delta^{15}N$ values were used to calculate the trophic positions of siphonophore species and particles. We used three approaches to estimate trophic position:

Trophic Position_{Glu-Phe} =
$$(\delta^{15}N_{Glu} - \delta^{15}N_{Phe}) - 3.4/7.6 + 1$$
, (1)

Trophic Position_{Ala-Phe} =
$$(\delta^{15}N_{Ala} - \delta^{15}N_{Phe}) - 3.2/5.7 + 1$$
, (2)

Trophic Position_{Tr-Src} =
$$(\delta^{15}N_{Tr} - \delta^{15}N_{Src}) - 3.6/5.7 + 1.$$
 (3)

Equation 1 relies on one trophic $(\delta^{15}N_{Glu})$ and one source $(\delta^{15}N_{Phe})$ amino acid, with a trophic discrimination factor of 7.6% and beta (β) of 3.4 following Chikaraishi et al. (2009). β represents the difference between source and trophic $\delta^{15}N$ values in primary producers and the trophic discrimination factor represents the ¹⁵N enrichment in trophic amino acids at each trophic step. Trophic discrimination factors can vary widely among taxa (McMahon and McCarthy 2016) and there are currently no published estimates for siphonophores. More recent studies have suggested that Eq. 2, which relies on alanine instead of glutamic acid, is more appropriate to estimate trophic positions in ecosystems with protistan consumers (Gutiérrez-Rodríguez et al. 2014; Décima et al. 2017). Eq. 3. which relies on a combination of multiple sources (averages of phenylalanine and lysine $\delta^{15}N$ values; $\delta^{15}N_{Src}$) and trophic amino acids (averages of leucine, glutamic acid, and alanine δ^{15} N values; δ^{15} N_{Tr}), a trophic discrimination factor of 5.7, and β of 3.6 % (Bradley et al. 2015).

Univariate linear models were used to examine the relationships between $\delta^{15}N_{Bulk}$ and $\delta^{15}N_{Phe}$ values and between source amino acid $\delta^{15}N$ values and collection depths. We tested for differences in source amino acid values and trophic positions between siphonophore genera using Analysis of Variance (ANOVA). We estimated and visualized the evolutionary history and phylogenetic distribution of trophic positions under a Brownian motion neutral divergence model using the package "phytools" and the topology of the molecular phylogeny in Damian-Serrano et al. (2021a). Recent work published by Damian-Serrano et al. (2021a,b) suggests that tentillum morphology is a primary driver of siphonophore diets. We used univariate linear models to examine the relationships between mean trophic positions calculated from CSIA-AA (this study) and tentilla characteristics from Damian-Serrano et al. (2021a).

Finally, we tested for temporal and geographic variability in $\delta^{15}N$ values. We used ANOVAs and Tukey's post hoc tests to test for differences in $\delta^{15}N$ values across years. This analysis was performed first with all siphonophore samples and then with siphonophore samples binned by suborder. Since there is high interspecific $\delta^{15}N$ variability in siphonophores, we also used ANOVAs to test for differences in $\delta^{15}N$ values over time for the three genera for which we had the highest sample sizes: *Apolemia, Bargmannia,* and *Nanomia*. To examine potential differences in $\delta^{15}N$ values between the sampling regions, we compared bulk $\delta^{15}N$ values between central and southern California using two-sample *t*-tests. There was only 1 yr where we sampled siphonophores in both regions (2020) and so we also tested for differences in $\delta^{15}N$ between regions in 2020. We compared the $\delta^{15}N_{Phe}$ and $\delta^{15}N_{Src}$ values of siphonophores

collected < 1500 m between the two regions. We excluded two samples that were collected > 2000 m (Monterey Bay) because we did not sample below the mesopelagic in southern California.

Results

$\delta^{15} N_{Bulk}$ and $\delta^{13} C_{Bulk}$ values

Siphonophore $\delta^{15}N_{Bulk}$ values ranged from 8.1‰ to 17.6‰, which represents approximately three trophic levels when assuming trophic enrichment of 3.4‰ (Post 2002). The mean \pm SD $\delta^{15}N_{Bulk}$ value across all siphonophores was 12.2‰ \pm 1.8‰, while $\delta^{13}C_{Bulk}$ values ranged from -23.3‰ to -16.7‰ with a mean \pm SD of -20.2‰ \pm 1.0‰ (Fig. 3A).

There were significant differences in $\delta^{15}N_{\rm Bulk}$ between siphonophores (ANOVA: $F_{(14,176)}=25.2$, p<0.00001), where Tukey's post hoc tests showed that 38 of 105 comparisons between species were significantly different. When genera were binned by suborder, we found significantly lower (t=9.1, df=169.8, p<0.000001) $\delta^{15}N_{\rm Bulk}$ values for calycophorans (mean: 10.9‰) compared to physonects (mean: 12.9‰). There were fewer significant differences in $\delta^{13}C_{\rm Bulk}$ values between siphonophore genera (ANOVA: $F_{(14,173)}=3.4$, p<0.0001) and no difference in $\delta^{13}C_{\rm Bulk}$ values between suborders (t=-0.6, df=117.2, p>0.1) (Fig. 3A).

Isotopic niches, inferred from Standard Ellipse Areas and corrected for sample size, were larger for physonects $(5.0\%^2)$ than calycophorans $(3.9\%^2)$. Furthermore, Bayesian Standard Ellipse Areas, which were calculated for each suborder, supported this finding (Fig. 3B; Supporting Information Table SM1). The 95% credible intervals for Bayesian Standard Ellipse Areas were $4.05.8\%^2$ for physonexts and $2.9-4.7\%^2$

for calycophorans. Hierarchical cluster analysis on bulk isotope values defined four clusters: group 1: *Erenna, Stephanomia*; group 2: *Bargmannia, Apolemia*, and *Lychnagalma*; group 3: *Vogtia, Diphyes, Nanomia*; group 4: *Chuniphyes, Frillagalma, Agalma, Sphaeronectes, Rosacea, Forskalia*, and *Praya* (Table 1). The agglomerative coefficient was 0.84, suggesting strong separation between groups.

Vertical gradients in $\delta^{15}N_{Bulk}$ values and relationships with environmental parameters

Siphonophore $\delta^{15}N_{Bulk}$ values significantly increased with increasing collection depth ($R^2=0.31$, $F_{(1,187)}=87.2$, p<0.000001). Similarly, $\delta^{15}N_{Bulk}$ values of sinking and suspended particles increased with depth, most notably for the smallest particle size class (Supporting Information Figure SM2). There were differences in siphonophore $\delta^{15}N_{Bulk}$ values when samples were binned into broad collection depths (epi-, meso-, and bathypelagic). Isotopic niches were larger in the mesopelagic and bathypelagic compared to the epipelagic (Fig. 3C; Supporting Information Table SM1). The 95% credible intervals for Bayesian Standard Ellipse Areas were 1.8–3.3‰² (epipelagic), 3.6–5.3‰² (mesopelagic), and 4.1–9.2‰² (bathypelagic). We found no relationship between siphonophore $\delta^{13}C_{Bulk}$ and collection depth ($R^2=0.01$, $F_{(1.175)}=3.6$, p=0.06).

The final model produced by backward and forward stepwise linear regression analyses showed that collection depth and latitude explained the most variability in $\delta^{15}N_{Bulk}$ values. Longitude and collection month did not improve the model fit. There was a large decrease in AIC from the intercept model to a model that included collection depth (174.3–137.8). The AIC was further reduced to 131.8 when latitude was included. The model fit was significantly improved

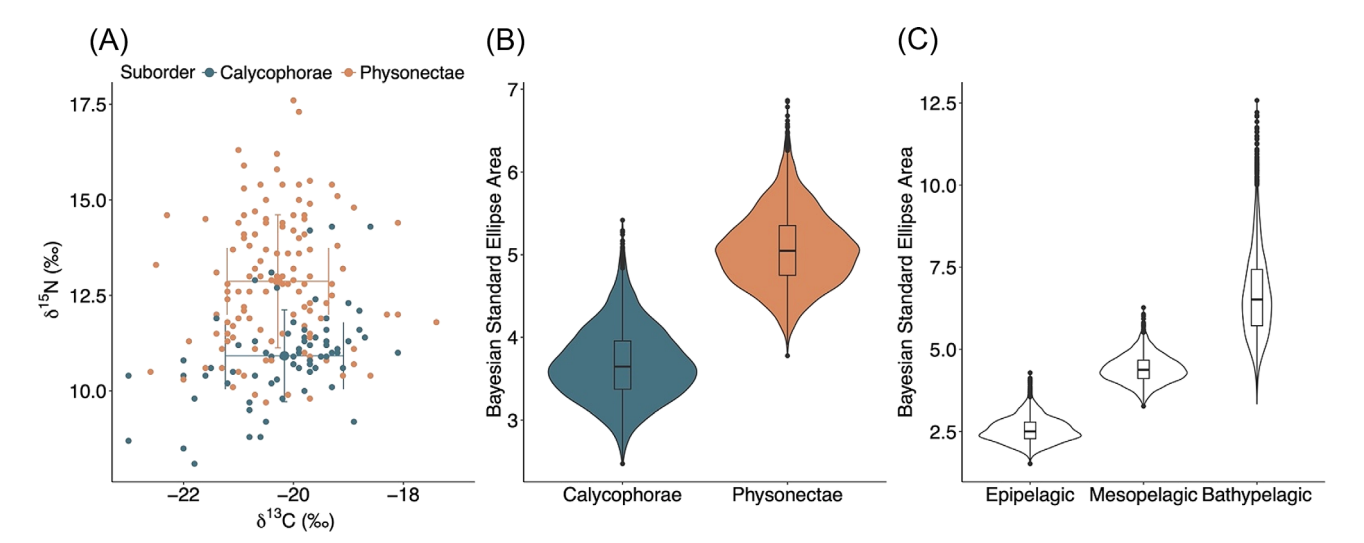


Fig. 3. (**A**) Bulk δ^{15} N and δ^{13} C values (‰) of siphonophores, color coded by suborder for Calycophorae (blue) and Physonectae (orange). Bars indicate standard error/deviation across each axis. (**B**) Bayesian isotopic niche widths estimated using standard ellipse areas (‰²) based on bulk δ^{15} N and δ^{13} C values of siphonophores. (**C**) Bayesian isotopic niche widths for samples collected in three depth habitats: epipelagic (0–200 m), mesopelagic (200–1000 m), and bathypelagic (> 1000 m). Boxplots show 95%, 75%, and 50% credible intervals.

Trophic ecology of siphonophores

 $(\chi^2 \text{ SS} = -18.3, p = 0.004)$ by the inclusion of depth and latitude compared to a depth-only model.

Temporal and spatial variability in $\delta^{15}N$ values

There was a significant difference in $\delta^{15}N_{Bulk}$ values over time $(F_{(1,200)} = 9.1, p = 0.002;$ Supporting Information Figure SM3), where $\delta^{15}N_{Bulk}$ values in 2021 were lower than most other years. This was driven by three samples of Rosacea, which had the lowest δ15N_{Bulk} values of all siphonophores analyzed in this study (Table 1) and were primarily collected only in 2021. Furthermore, all 2021 samples were of calycophorans, which have lower δ¹⁵N_{Bulk} values than physonects. When samples were grouped by siphonophore suborders, there were no differences in $\delta^{15} N_{Bulk}$ values over our sampling period (p = 0.12 for physonects; p = 0.07 for calycophorans). In addition, there were no differences in $\delta^{15}N_{Bulk}$ values over time for each of the three genera for which we have numerous samples across years (Apolemia, Bargmannia, and *Nanomia*; p > 0.2 for all ANOVAs; Supporting Information Figure SM4). Finally, there was no difference in $\delta^{15}N_{Src}$ values over our sampling period ($F_{(1,31)} = 0.07$, p = 0.79).

There was no difference in $\delta^{15} N_{Bulk}$ values between samples collected off southern vs. central California (t=1.88, df = 200, p=0.06). Similarly, there were no regional differences in $\delta^{15} N_{Bulk}$ values when we only compared $\delta^{15} N_{Bulk}$ values of siphonophores that were collected in both regions in 2020 (t=1.39, df = 58, p>0.1; Fig. 2). Finally, there were no differences in the $\delta^{15} N_{Src}$ values of siphonophores between central and southern California waters (t=1.72, df = 29, p=0.1).

CSIA-AA

There was a positive relationship between $\delta^{15}N_{Bulk}$ and $\delta^{15}N_{Src}$ values of siphonophores ($R^2=0.22$, $F_{(1,31)}=10.2$, p=0.003) and particles ($R^2=0.62$, $F_{(1,19)}=33.5$, p<0.00001) suggesting that $\delta^{15}N_{Src}$ values could explain some variation in $\delta^{15}N_{Bulk}$ values (Fig. 4). $\delta^{15}N_{Src}$ values of siphonophores ranged from 6.7% to 11.3% (Fig. 4). There was no difference in $\delta^{15}N_{Src}$ values between siphonophore suborders (t=0.5, df = 14.4, p>0.1). The mean \pm SD $\delta^{15}N_{Src}$ value for calycophorans was 7.9% \pm 1.5% compared to 8.2% \pm 1.0% for physonects and the range was comparable between suborders (calycophorans range = 4.7%; physonect range = 4.0%).

There were no differences in trophic position estimates derived from the three different equations for particles, but there were differences in siphonophore trophic position estimates between methods (Supporting Information Table SM2). Siphonophore trophic positions calculated using a single source and trophic amino acid (Trophic Position $_{\text{Glu-Phe}}$; Eq. 1) following Chikaraishi et al. (2009) ranged from 2.4 to 4.2 (mean = 3.2). Trophic positions estimated using a combination of source and trophic amino acids (Trophic Position $_{\text{Tr-Src}}$; Eq. 3) following Bradley et al. (2015) ranged from 2.4 to 4.0 (mean = 3.0) (Supporting Information Table SM2). The differences in trophic position estimates between methods were not

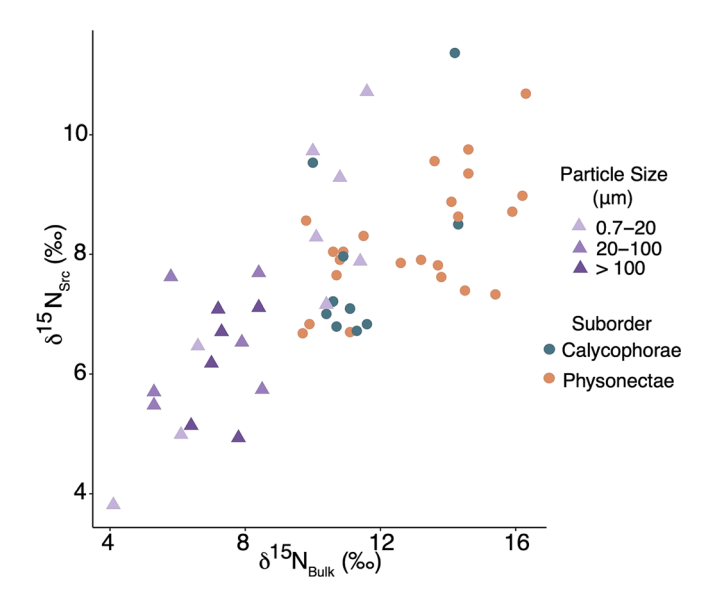


Fig. 4. Positive relationships between the $\delta^{15}N$ values of bulk tissue $(\delta^{15}N_{Bulk})$ and source amino acids $(\delta^{15}N_{Src})$ for siphonophores (circles) and three size classes of particles (triangles).

significant (t = -1.7, df = 64, p = 0.10). However, Trophic Position_{Ala-Phe} (Eq. 2) produced higher siphonophore trophic positions, ranging from 2.5 to 4.8, with a mean of 3.5 (Supporting Information Figure SM5; Supporting Information Table SM2). Since alanine is included Eq. 3 (Trophic Position_{Tr-Src}), this equation was used for the remainder of our analyses because it accounts for trophic steps that include both protists and zooplankton (Hannides et al. 2020).

Overall, trophic positions spanned nearly two trophic levels, suggesting diet differences between siphonophore species (Fig. 5). Siphonophores with lower trophic positions were a mixture of calycophoran and physonect species, whereas all siphonophores with higher trophic positions were physonects (Fig. 5). Trophic Position_{Tr-Src} for physonects ranged from 2.6 to 4.0 with a mean of 3.2. They were significantly higher (t = 3.4, df = 25.6, p = 0.001) than calycophoran trophic positions, which ranged from 2.4 to 3.0 with a mean of 2.7. Chuniphyes sp. had the lowest trophic position (mean = 2.6) and Bargmannia spp. had the highest trophic position estimate (mean = 3.5) (Fig. 5; Supporting Information Table SM2). We found few significant relationships between siphonophore trophic position and tentillum morphological traits, except for heteroneme width $(R^2 = 0.40, F_{(1,8)} = 7.1, p = 0.02)$, which increased with increasing trophic position (Supporting Information Figure SM6).

There was a strong positive relationship between siphonophore $\delta^{15}N_{Src}$ values and siphonophore collection depth $(R^2=0.40,\,F_{(1,31)}=21.2,\,p<0.00001;\,\mathrm{Fig.~6A})$. Similarly, $\delta^{15}N_{Src}$ values of particles increased from 0 to 500 m (Fig. 6B). However, there was no relationship between trophic position and collection depth for siphonophores $(R^2=0.03,\,F_{(1,31)}=2.1,\,p>0.1;\,\mathrm{Fig.~6C})$. Surface particles (< 50 m collection depth) of

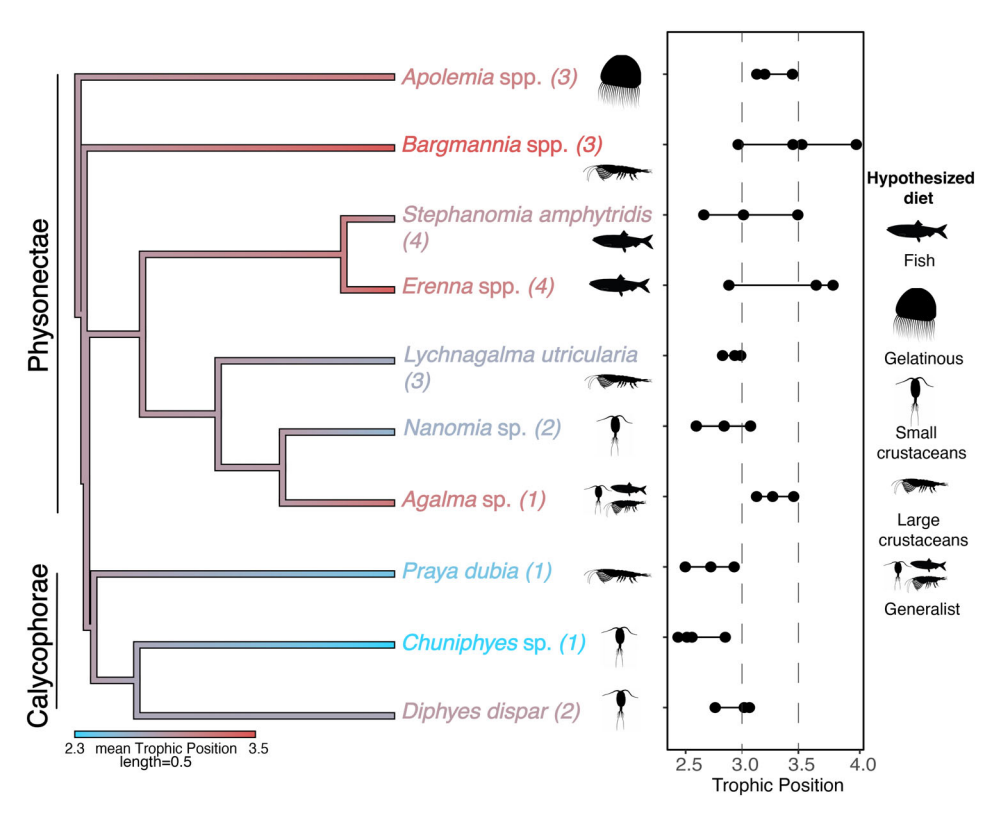


Fig. 5. Molecular phylogeny subset derived from the topology in Damian-Serrano et al. (2021*a*), measured trophic position, and hypothesized siphonophore diet derived from previous diet studies (reviewed by Hetherington et al. 2022*b*). The subset phylogeny only includes species analyzed for CSIA-AA in this study. Trophic positions (Eq. 3) were derived from CSIA-AA, where means are depicted by color (left panel), and ranges are plotted in the right panel. Numbers in parentheses represent the cluster number from a hierarchical cluster analysis based on bulk carbon and nitrogen isotope values (this study). Hypothesized diets were obtained from the literature (references in main text).

all size classes had lower $\delta^{15} N_{Src}$ values (median = 5.1‰) than deeper particles (median = 7.1%) (Supporting Information Table SM3). While there were no differences in $\delta^{15}N_{Src}$ between particle sizes at the surface, $\delta^{15}N_{Src}$ values of small deep particles were higher (median 8.3%) than those of larger deep particles (6.7‰) (Fig. 7; Supporting Information Table SM3). The $\delta^{15}N_{Src}$ values of siphonophores, which ranged from 6.7% to 11.4%, suggest feeding across surface and deep baselines. Some epipelagic siphonophores more closely overlapped with surface or large (sinking) particle δ¹⁵N_{Src} values (e.g., Agalma sp., Diphyes dispar) (Fig. 7). The highest $\delta^{15}N_{Src}$ values were found in deeppelagic siphonophores (Erenna spp., Lychnagalma utricularia, Chuniphyes moserae). These values overlapped more closely with deep, small (suspended) particles (range 6.5%-10.7%) than surface or larger particles (Fig. 7; Supporting Information Table SM3).

Discussion

Using CSIA-AA, we identified the sources of siphonophore food web baselines (i.e., surface vs. deep large and small particles), disentangled the influence of baseline vs. trophic variability, and estimated siphonophore trophic position.

Increases in δ^{15} N values with increasing depth for both siphonophores and particles suggest that that microbially reworked particles are likely an important food source for primary consumers in the deep pelagic. Our results show that siphonophore trophic positions span ~ 1.5 trophic levels and there are clear differences in $\delta^{15}N$ values and trophic positions between siphonophore species. While $\delta^{15} N_{\text{Bulk}}$ values differed between depths, we found no difference in siphonophore trophic positions between epi- and deep-pelagic habitats. Isotope values and trophic positions suggest high trophic overlap between calycophoran and physonect siphonophores at lower trophic levels. Siphonophores that feed at higher trophic levels, however, were restricted to deep-pelagic physonect species. This suggests that deep-pelagic siphonophores may exhibit more niche partitioning than epipelagic ones. Altogether, this study illustrates the value of isotopic tracers in midwater food web studies, the trophic diversity of siphonophores and the complexity of food web structure in the deep pelagic.

Siphonophore dietary niches inferred from bulk isotope values

Siphonophore $\delta^{15}N_{Bulk}$ values were highly variable (range = 8.8%), suggesting that they feed across multiple trophic

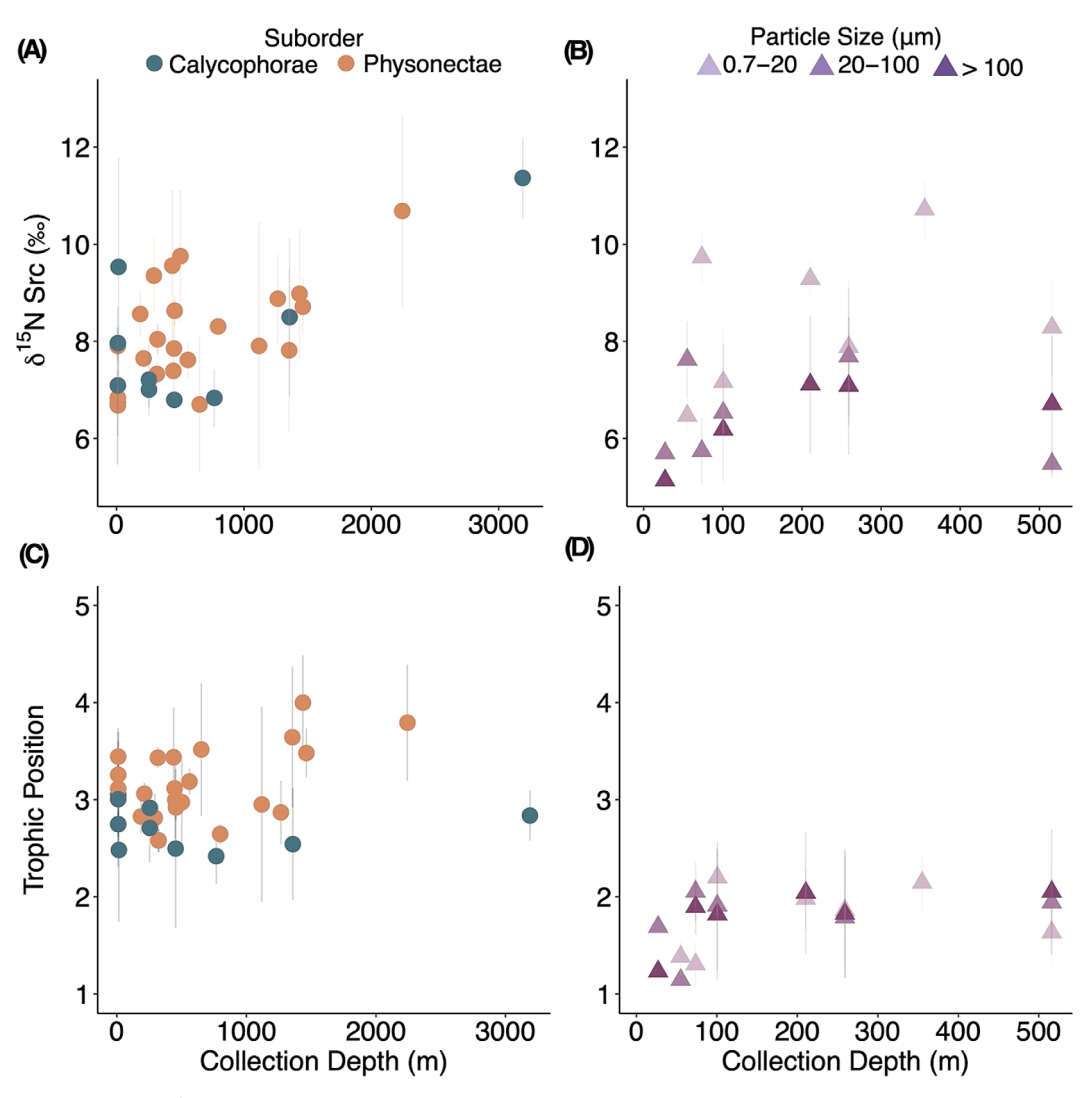


Fig. 6. Relationships between (**A**) $\delta^{15}N_{Src}$ values of siphonophores and (**B**) particles and collection depths, (**C**) Trophic Position_{Tr-Src} of siphonophores and (**D**) particles and their collection depths. Error bars represent propagated errors, which were calculated following Bradley et al. (2015).

levels in the pelagic ocean. A distinction between physonect and calycophoran isotope values was evident in our dataset (Fig. 3). While there was substantial overlap between calycophoran and physonect $\delta^{13}C$ and $\delta^{15}N$ values, physonects had larger overall ranges and higher mean and maximum $\delta^{15}N_{Bulk}$ values. This suggests that calycophorans are restricted to lower trophic positions and their diets are generally less variable than physonects. Some physonect (e.g., *Cordagalma*) $\delta^{15}N_{Bulk}$ values overlap with calycophorans. However, other physonect species (e.g., *Erenna*, *Bargmannia*) had higher $\delta^{15}N_{Bulk}$ values, suggesting the consumption of higher trophiclevel prey.

Compared to physonects, calycophoran tentilla, are more structurally homogeneous (Damian-Serrano et al. 2021b). This may suggest that collectively their diets are less varied than physonects, where calycophorans are mostly preying on small crustaceans. The larger overall range in physonect $\delta^{15} N_{\rm Bulk}$

values suggests that physonects may exhibit more niche partitioning, with individual species relying on different prey resources. This supports recent work suggesting a high degree of specialization in deep-pelagic physonect species (Hetherington et al. 2022b).

Interspecific differences in $\delta^{15}N_{Bulk}$ values between physonect species support previous hypotheses suggesting that physonects have carved out distinct dietary niches in the deep pelagic. Siphonophore species clustered into four depth-associated trophic groups, which can be interpreted in the context of the limited previous information on siphonophore trophic ecology. Groups 1 and 2 included mostly larger, deeper-dwelling physonect siphonophores. Group 1 consisted of *Erenna* and *Stephanomia*. Previous ROV observations indicate that *Erenna* species consume fish. There are no published gut contents analysis data for *Stephanomia*, although it is notable that *Stephanomia* and *Erenna* bear the largest tentilla of

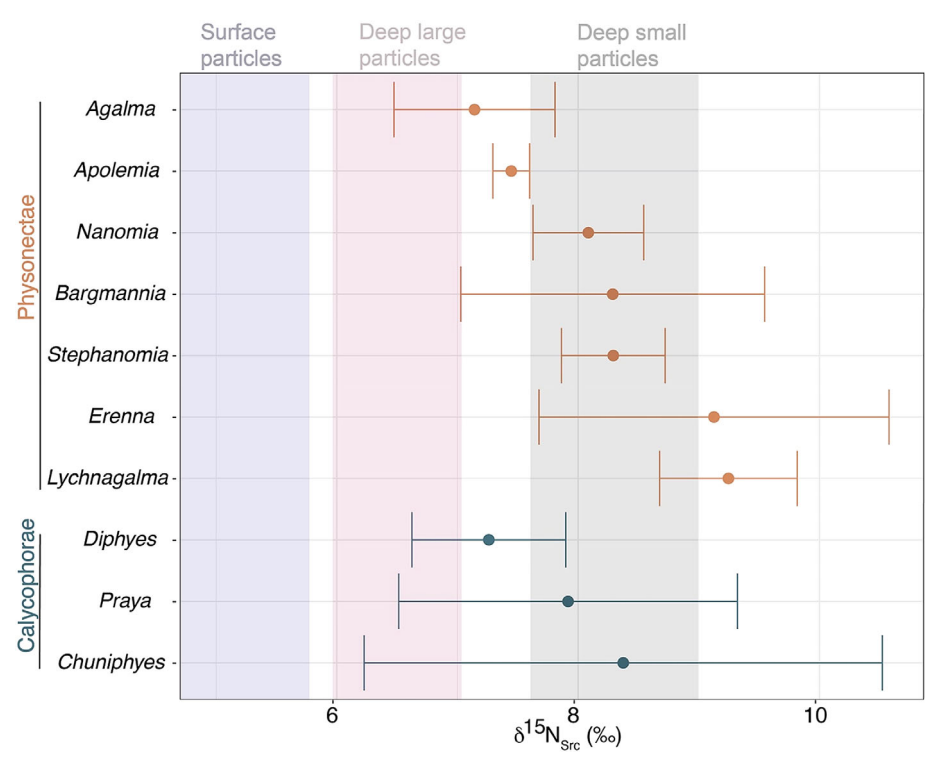


Fig. 7. Mean and standard deviations of $\delta^{15}N$ values of source amino acids ($\delta^{15}N_{Src}$) for siphonophore genera, grouped by suborder. Vertical bars (from left to right) represent the mean \pm SD $\delta^{15}N_{Src}$ values of surface (0–50 m; all sizes) particles (lavender, far left), deep large/sinking particles (pink, center), and deep small/suspended particles (gray, right) collected in Monterey Bay in summer.

siphonophore species (Damian-Serrano et al. 2021a), and perhaps they are similarly able to capture larger fish prey than other siphonophore species. Group 2 consisted of *Bargmannia*, *Apolemia*, and *Lychnagalma*, species for which there are no published gut contents analysis data. The $\delta^{15}N$ and $\delta^{13}C$ values of species in Group 2 suggest that these deeperdwelling physonect species feed at a similar trophic position and/or in overlapping depth habitats. Compared to other siphonophores in this study, species in groups 1 and 2 likely feed at higher trophic levels than groups 3 and 4, as their $\delta^{15}N$ values were higher than other species we sampled.

The third cluster (*Vogtia serrata*, *Diphyes dispar*, and *N. bijuga*) comprised two calycophorans species and a physonect, *N. bijuga*. Isotope values generally suggest that cluster 3 species are feeding on lower trophic level taxa, likely small crustaceans. This supports previous diet studies (Purcell 1981a; Damian-Serrano et al. 2022), which identified copepods, ostracods, and other small crustaceans as prey items. The fourth cluster (*Agalma, Sphaeronectes, Frillagalma, Forskalia, Chuniphyes, Rosacea*, and *Praya*) also includes both calycophorans and physonects. This group appears to include species that may exhibit wider diet diversity and are primarily epipelagic, except for *Chuniphyes*, which includes the deeperdwelling species *C. moserae*. The sample sizes for species in this cluster were mostly smaller than sample sizes for other taxa, except for *Chuniphyes*. It is possible that the full isotopic

ranges of these species were not determined for some species given the limited sample sizes.

Our results suggest that siphonophore suborder, depth, and possible size and/or morphology are informative for understanding siphonophore trophic ecology. It is unclear whether prey type and size are correlated with siphonophore colony size. Unlike many taxa, siphonophores are not gape limited, with mouths and stomachs that can stretch several times their size (Pagès and Madin 2010). Moreover, they have many feeding bodies (gastrozooids) along the lengths of the colony. It is notable, however, that large physonect species were in clusters 1 and 2 and smaller calycophorans were primarily in clusters 3 and 4. Future studies that examine colony size, gastrozooid size and/or morphology in relation to diet would provide insight into the relationship between siphonophore and prey size.

Trophic clustering is also likely influenced by similarities in siphonophore swimming behavior and colony size, which varies among species, and impacts feeding. While all siphonophores are passive sit-and-wait ambush predators, some are more likely to track small-scale prey aggregations than others. Many diphyid calycophorans (clusters 3 and 4) are small, strong swimmers that are hypothesized batch feeders that prey on small crustaceans (2004). Larger siphonophores, including some of the deeppelagic physonects in this study (e.g., *Erenna, Stephanomia*; cluster 1), and some larger calycophorans (e.g., *Praya, Rosacea*; cluster

4) feed more passively, waiting for prey to bump into their tentacles (Purcell 1981a). Prey availability, which is often patchily distributed and varies spatially, also influences trophic ecology. Future studies that investigate how siphonophore diets are shaped by swimming behavior and colony size, would be useful for identifying trophic clusters and partitioning among species.

Siphonophore trophic positions

The difference in trophic position estimates between calculation methods (Eqs. 1, 3) was small and not statistically significant, where Trophic $\operatorname{Position_{Glu-Phe}}$ (Eq. 1) and Trophic $\operatorname{Position_{Tr-Src}}$ (Eq. 3) yielded almost identical values (Supporting Information Table SM2). Trophic Position_{Ala-Phe} (Eq. 2) estimates, however, were higher (on average, 0.5) than Trophic Position_{Glu-Phe} or Trophic Position_{Tr-Src} (Supporting Information Figure SM5; Supporting Information Table SM2). Higher trophic position estimates using Eq. 2 indicates the contribution of protists and the microbial loop in this food web. Trophic Position_{Tr-Src} was ultimately used for most analyses because it uses multiple source and trophic amino acids and accounts for both trophic steps that include protists and zooplankton (Hannides et al. 2020).

Overall, Trophic Position_{Tr-Src} ranged between 2.2 and 4.0 (Fig. 5). There was high overlap in trophic position between calycophorans and physonects, with species from both suborders feeding at lower trophic positions. Species from both suborders had lower trophic positions but higher trophic positions were restricted to deep-pelagic physonect species. This supports the findings from molecular gut content analyses across depth habitats in Damian-Serrano et al. (2022), showing that small hard-bodied prey are consumed by siphonophores in both shallow and deep habitats. However, the highest siphonophore trophic positions were physonect species (*Erenna, Bargmannia, Apolemia*), which aligns with previous studies indicating that they feed on larger, higher trophic level species, compared to other siphonophore species.

There were clear relationships between siphonophore trophic positions and phylogeny, suggesting that trophic niches can be partially explained by evolutionary history (Fig. 5). Siphonophores are classified into three suborders: Cystonectae (not included in this study) lack heteroneme nematocysts and are well-known piscivores. Cystonects are the sister group to Codonophora, which is the clade composed of the paraphyletic suborder Physonectae, within which the derived suborder Calycophorae is nested (Munro et al. 2018). Previous work suggests that ancestral siphonophores specialized on large, soft-bodied prey and subsequently went through several evolutionary transitions in which siphonophore tentilla and diet diversified (Damian-Serrano et al. 2021a,b). Some of these species (in clade A physonects and Calycophorae) evolved to specialize on small, hard-bodied prey, and others evolved generalist niches. This transition to lower trophic level prey may have presented evolutionary advantages, as clade

physonects and Calycophorae are the most speciose and abundant extant siphonophores.

The phylogenetic distribution of trophic positions in our results (Fig. 5) suggest that the most recent common ancestor of Codonophora had a high trophic position, which is retained in the high trophic positions of Bargmannia, Apolemia, and Erenna. The species with lower trophic positions are in all clade A or Calycophorae, which reflects two independent evolutionary transitions to feeding at lower trophic levels. This finding is supported further by the distribution of evolutionary regimes of siphonophore tentilla in Damian-Serrano et al. (2021b), where they identified two instances of convergent evolution of tentillum morphology across clade A and Calycophorae. Our work supports the conclusions of Damian-Serrano et al. (2021a) suggesting that both siphonophore specialists and generalists have evolved from specialist ancestors by modifying their tentilla. Integrating evolutionary history to present day diet analyses provides greater context for the diversity of siphonophore trophic niches in the pelagic ocean.

In this study, we used published morphology data on a subset of species that we sampled for stable isotope analysis. There was a significant positive relationship between trophic positions and one trait (heteroneme width; Supporting Information Figure SM6), suggesting that siphonophores with higher trophic positions have wider nematocysts, which may allow them to capture larger prey. Future studies that directly measure siphonophore traits from colonies that are also used for stable isotope and/or gut content analyses would provide further insights into how tentillum morphology shapes siphonophore feeding ecology.

Trophic position estimates and stable isotope caveats

Relative to other CSIA-AA literature, the span of ~ 1.5 trophic positions is ecologically reasonable for siphonophores. Calycophorans, for example, primarily consume smaller crustaceans (e.g., copepods, ostracods) (Purcell 1981a; Damian-Serrano et al. 2022). Décima et al. (2013) used CSIA-AA on the copepod *Calanus pacificus* in the California Current Ecosystem and estimated their Trophic Position_{Glu-Phe} as 1.8 to 2.5. While this study was conducted at a different time, during the 1997–1998 El Niño and La Niña periods, it suggests that copepod trophic positions are lower than calycophorans (Trophic Position_{Glu-Phe} range = 2.5–3.6), which is expected if calycophorans are consuming copepods.

CSIA-AA can underestimate absolute trophic positions compared to other methods (e.g., diet analysis) that are used to estimate trophic position. Previous studies have demonstrated that the widely-used trophic discrimination of 7.6% (Eq. 1) is an overestimate for many higher trophic level species (Bradley et al. 2015; McMahon and McCarthy 2016; Hetherington et al. 2017) and results in an underestimation in trophic position (Germain et al. 2013; Bradley et al. 2015; McMahon and McCarthy 2016). Thus, it is possible that the absolute

Trophic ecology of siphonophores

siphonophore trophic positions presented here are underestimated. We recognize that there is no published estimate of siphonophore trophic discrimination factors, which vary widely among consumers. Feeding experiments that measure ¹⁵N enrichment between siphonophores and their diets are needed to explicitly quantify trophic discrimination. This would require rearing siphonophores in the laboratory. This is logistically challenging and there are few examples of culturing siphonophores in the literature. In one recent study (Patry et al. 2020), the authors successfully cultured the abundant physonect N. bijuga and describe an effective methodology for culturing gelatinous zooplankton, which could be useful for conducting feeding experiments, to estimate siphonophore trophic descrimination. Stable isotope values provide a timeintegrated perspective of diet. The time frame represented by these values is based on tissue turnover, which is also largely unknown for gelatinous zooplankton. A recent study found the δ¹⁵N_{Bulk} half life of *Chrysaora pacifica*, a scyphozoan, was 35.6 d (Schaub et al. 2021) but there are no published estimates for siphonophore tissue turnover. Future feeding experiments would therefore be instrumental in addressing the assumptions and caveats associated with stable isotope analyses and trophic position estimates.

It is also possible that $\operatorname{Trophic}$ Position_{Glu-Phe} values are underestimates because it fails to capture trophic transfers in the lower portion of the food web. Glutamic acid (trophic amino acid) shows little enrichment and a "trophic invisibility" with protistan trophic transfers. Thus, when glutamic acid is used, trophic positions may be underestimated in ecosystems with protistan grazers (Gutiérrez-Rodríguez et al. 2014; Landry and Décima 2017). These studies indicate that alanine, unlike glutamic acid, exhibits trophic enrichment with protistan and zooplankton trophic steps. For siphonophores in this study, $\operatorname{Trophic}$ Position_{Ala-Phe} estimates were higher (on average, 0.5) than $\operatorname{Trophic}$ Position_{Glu-Phe} or $\operatorname{Trophic}$ Position_{Tr-Src} (Supporting Information Figure SM5; Supporting Information Table SM2).

Higher Trophic Position Ala-Phe values in comparison to Trophic Position_{Glu-Phe} may suggest a considerable contribution of heterotrophic protists in the planktonic food web. Bode et al. (2021) suggest substantial links between microbial and metazoan food webs in midwater micronekton taxa (mostly fishes). Accounting for microbial steps in the food web increased the trophic positions of midwater fishes by 0.5-0.8 (Bode et al. 2021). Similarly, Shea et al. (2023) found that in the epipelagic and upper mesopelagic, protistan microzooplankton are substantial components of the food web supporting higher zooplankton trophic levels. Our results support their hypothesis that microbial contributions to micronekton are especially important in the deep pelagic where photosynthesis does not occur, and microbial reworking of organic matter is important for fueling midwater food webs. However, further studies are needed to examine the mechanisms driving differences in enrichment between trophic amino acids and the degree to which alanine can be used to quantify microbial steps in the food web.

Temporal and spatial $\delta^{15}N$ dynamics

We found strong relationships between $\delta^{15}N_{Bulk}$ and $\delta^{15}N_{Src}$ values of siphonophores and collection depth (Fig. 6). Niche width estimates from bulk isotope values differed between siphonophore suborders and depth habitats, where niche widths were greater in the meso- and bathypelagic compared to the epipelagic (Fig. 3). There are several possible hypotheses to explain this pattern. First, our results could suggest that siphonophores in the deep pelagic have evolved unique dietary niches to partition resources in a habitat where prey abundances are low and/or variable. Second, isotopic ellipse areas may have been smaller in the epipelagic because these values are derived from species with restricted depth habitats that do not vertically migrate. In contrast, the deeppelagic samples included species that perhaps have more varied niches because they may consume prey at depth during the day, in surface waters at night, or prey on vertically migrating zooplankton; or because most epipelagic prev feeds on an isotopically similar basal trophic level (e.g., phytoplankton). Finally, it is possible that the differences are not related to siphonophore dietary niches but reflect differences in baseline $\delta^{15}N$ values that affect consumer $\delta^{15}N$ values. Particle data from Monterey Bay support the last hypothesis, where changes in isotopic baselines contributed to variability in siphonophore δ^{15} N values (Figs. 6, 7).

Previous studies in the North Pacific Subtropical Gyre demonstrated increases in the $\delta^{15}N$ values of particulate organic matter, zooplankton, and micronekton with increasing depth (Hannides et al. 2013; Choy et al. 2015; Gloeckler et al. 2018; Hannides et al. 2020). In those studies, the ¹⁵N enrichment in the mesopelagic was attributed to the microbial degradation of suspended particles at depth (Saino and Hattori 1980; Casciotti et al. 2008). It has been hypothesized that ¹⁵N enrichment is driven by cleavage of ¹⁴N peptide bonds during organic matter degradation (Hannides et al. 2013; Yamaguchi and McCarthy 2018). When zooplankton and micronekton have higher $\delta^{15}N_{Src}$ values in the mesopelagic compared to epipelagic, it therefore can suggest a shift in nutritional sources from surface derived material to large (sinking) or small (suspended) particles (Hannides et al. 2013; Choy et al. 2015; Romero-Romero et al. 2020).

Here, we compare siphonophore data spanning multiple locations and sampling times in the California Current Ecosystem to particles collected at a single time and location in Monterey Bay. Nonetheless, the particle data illustrate a similar pattern as what has been reported at other open-ocean sites (Station ALOHA and Station Papa: Gloeckler et al. 2018; Wojtal et al. 2023): an increase in both bulk and source amino acid $\delta^{15}N$ values with depth for smaller particles, but not large particles (Supporting Information Figure SM2). Overall, smaller particles had higher $\delta^{15}N$ values than larger particle sizes and increased with depth (Supporting Information Figure SM2; Supporting Information Table SM3). These results agree with previous studies indicating that smaller particles

are exposed to more microbial degradation than larger particles which sink faster through the water column.

Relationships between $\delta^{15}N$ values and collection depth of metazoans have been documented in the North Pacific Subtropical Gyre (Choy et al. 2015; Gloeckler et al. 2018), Gulf of Mexico (Richards et al. 2020), and Atlantic (Parzanini et al. 2017) and have been attributed, in part, to reliance of the deep food web on deep, degraded particles. Here, our siphonophore $\delta^{15}N_{Phe}$ and $\delta^{15}N_{Src}$ values also increased with increasing depth in a sample set that spans several collection times and locations, suggesting that siphonophores in the deep-pelagic feed on prey within a food web that is partially supported by deep small particles. The $\delta^{15}N_{Src}$ values of siphonophores were highly variable across samples, genera, and collection depths, which suggests that siphonophores are linked both to surface (fresh) and deeper (microbially degraded) food web baselines (Fig. 7). Lower $\delta^{15}N_{Src}$ values for some genera (e.g., Agalma, Diphyes, Chuniphyes) suggest that their prey feed on epipelagic organic matter and/or large sinking particles. The $\delta^{15}N_{Src}$ values of most siphonophore samples were higher than surface and large particle $\delta^{15}N_{Src}$ values, suggesting some indirect reliance on deeper particles (Fig. 7). The $\delta^{15}N_{Src}$ values from some siphonophore samples, mostly from deeperdwelling physonects (Erenna, Lychnagalma) were higher than deep small particle $\delta^{15}N_{Src}$ values. Small particles are a heterogeneous mixture of sizes and composition. These siphonophores are predators of zooplankton and micronekton, but they may be indirectly relying on a subset of these particles. Particles that are exposed to more microbial degradation and have even higher $\delta^{15} N_{Phe}$ and $\delta^{15} N_{Src}$ values compared to the rest of the particle pool, are consumed by lower trophic level taxa and ultimately support siphonophores and the remainder of the food web. This conclusion is similar to those drawn by previous studies focused on different taxa (Gloeckler et al. 2018; Hannides et al. 2020; Shea et al. 2023).

The range in siphonophore $\delta^{15}N_{Phe}$ and $\delta^{15}N_{Src}$ values was lower in the epipelagic than deep-pelagic species (Supporting Information Table SM3). Deep-pelagic siphonophores may utilize a wider range of basal resources, with some species feeding in the epipelagic or on vertically migrating prey and others relying more on deep small particle baselines. Some species, like Agalma elegans and Praya dubia, Stephanomia amphytridis, and N. bijuga showed little variation in $\delta^{15}N_{Src}\sim 1\%$ while others, like Bargmannia spp. and Chuniphyes sp., had larger ranges (2.9% and 4.6%, respectively). Similarly, this could suggest that species with higher ranges are accessing food resources in epipelagic and deep-pelagic habitats. Given the broad depth range in our Bargmannia spp. and Chuniphyes sp. samples (Supporting Information Figure SM1), our sampling likely captured multiple species within each genus that inhabit distinct vertical zones.

The $\delta^{15}N$ values of consumers are ultimately governed by N-cycling and ocean biogeochemistry, which vary spatially, temporally, and vertically (Hannides et al. 2009; Choy

et al. 2015; Close 2019). Although our study represents the most comprehensive bulk δ^{15} N, and the first CSIA-AA, dataset for siphonophores, we recognize that baseline and consumer δ^{15} N values are spatiotemporally variable within the dynamic California Current Ecosystem (Rau et al. 1998; Miller et al. 2013; White et al. 2022; Supporting Information Figure SM7). Siphonophores were collected over several years and locations in the California Current Ecosystem and particles were collected from one location and time point in Monterey Bay.

Our study provides a snapshot of particle $\delta^{15}N$ dynamics in Monterey Bay in the late summer. These dynamics likely change as phytoplankton utilization of nitrate relative to supply and particle flux change throughout the year in the California Current Ecosystem (Rau et al. 1998; Miller et al. 2013; Shen et al. 2021; White et al. 2022). Bulk and source amino acid δ¹⁵N values of siphonophores did not change significantly over time or between regions. Furthermore, the particle $\delta^{15}N$ data are within the ranges of other $\delta^{15}N$ particle data from the region (Supporting Information Figure SM7). However, future sampling in the central and southern California Current Ecosystem over multiple seasons and years would be needed to comprehensively examine seasonal patterns in baseline $\delta^{15}N$ values. The Monterey Bay and the larger California Current Ecosystem is a highly dynamic region, where fronts and other oceanographic features influence the sinking rates of particles. For example, density gradients have been shown to affect the settling velocities of particles (Prairie et al. 2015). Under certain conditions, particles may remain in surface waters for longer time and thus be exposed to more microbial degradation. Our sampling approach did not capture these fine-scale particle-siphonophore dynamics. Future research that samples particles, prey, and siphonophores across different frontal systems could provide insight into how these oceanographic features impact food web structure and predator trophic ecology.

Data availability statement

All isotopic values (siphonophores and particles) and sample information from this study are available through the Biological & Chemical Oceanography Data Management Office (BCO-DMO) (https://www.bco-dmo.org/project/738543).

References

Biggs, D. C. 1977. Field studies of fishing, feeding, and digestion in siphonophores. Mar. Behav. Physiol. **4**: 261–274. doi:10.1080/10236247709386958

Bishop, J. K. B., P. J. Lam, and T. J. Wood. 2012. Getting good particles: Accurate sampling of particles by large volume insitu filtration. Limnol. Oceanogr.: Methods **10**: 681–710. doi:10.4319/lom.2012.10.681

Bode, A., M. P. Olivar, and S. Hernández-León. 2021. Trophic indices for micronektonic fishes reveal their dependence on

- the microbial system in the North Atlantic. Sci. Rep. **11**: 8488. doi:10.1038/s41598-021-87767-x
- Bradley, C. J., N. J. Wallsgrove, C. A. Choy, J. C. Drazen, E. D. Hetherington, D. K. Hoen, and B. N. Popp. 2015. Trophic position estimates of marine teleosts using amino acid compound specific isotopic analysis. Limnol. Oceanogr.: Methods **13**: 476–493. doi:10.1002/lom3.10041
- Brodeur, R. D., T. D. Auth, and A. J. Phillips. 2019. Major shifts in pelagic micronekton and macrozooplankton community structure in an upwelling ecosystem related to an unprecedented marine heatwave. Front. Mar. Sci. **6**: 212. doi:10. 3389/fmars.2019.00212
- Cardona, L., I. Álvarez de Quevedo, A. Borrell, and A. Aguilar. 2012. Massive consumption of gelatinous plankton by Mediterranean apex predators. PloS One **7**: e31329. doi:10. 1371/journal.pone.0031329
- Casciotti, K. L., T. W. Trull, D. M. Glover, and D. Davies. 2008. Constraints on nitrogen cycling at the subtropical North Pacific Station ALOHA from isotopic measurements of nitrate and particulate nitrogen. Deep-Sea Res. II Top. Stud. Oceanogr. **55**: 1661–1672. doi:10.1016/j.dsr2.2008. 04.017
- Chi, X., and others. 2021. Tackling the jelly web: Trophic ecology of gelatinous zooplankton in oceanic food webs of the eastern tropical Atlantic assessed by stable isotope analysis. Limnol. Oceanogr. **66**: 289–305. doi:10.1002/lno.11605
- Chikaraishi, Y., and others. 2009. Determination of aquatic food-web structure based on compound-specific nitrogen isotopic composition of amino acids. Limnol. Oceanogr.: Methods **7**: 740–750. doi:10.4319/lom.2009.7.740
- Choy, C. A., B. N. Popp, C. C. S. Hannides, and J. C. Drazen. 2015. Trophic structure and food resources of epipelagic and mesopelagic fishes in the North Pacific Subtropical Gyre ecosystem inferred from nitrogen isotopic compositions. Limnol. Oceanogr. **60**: 1156–1171. doi:10.1002/lno. 10085
- Choy, C. A., S. H. D. Haddock, and B. H. Robison. 2017. Deep pelagic food web structure as revealed by *in situ* feeding observations. Proc. R. Soc. B Biol. Sci. **284**: 20172116. doi: 10.1098/rspb.2017.2116
- Close, H. G. 2019. Compound-specific isotope geochemistry in the ocean. Ann. Rev. Mar. Sci. **11**: 27–56. doi:10.1146/annurev-marine-121916-063634
- Condon, R. H., and others. 2012. Recurrent jellyfish blooms are a consequence of global oscillations. Proc. Natl. Acad. Sci. U.S.A. **110**: 1000–1005. doi:10.1073/pnas.1210920110
- Damian-Serrano, A., S. H. D. Haddock, and C. W. Dunn. 2021*a*. The evolution of siphonophore tentilla for specialized prey capture in the open ocean. Proc. Natl. Acad. Sci. **118**: e2005063118. doi:10.1073/pnas.2005063118
- Damian-Serrano, A., S. H. D. Haddock, and C. W. Dunn. 2021*b*. The evolutionary history of siphonophore tentilla:

- Novelties, convergence, and integration. Integr. Org. Biol. **3**: obab019. doi:10.1093/iob/obab019
- Damian-Serrano, A., E. D. Hetherington, C. A. Choy, S. H. Haddock, A. Lapides, and C. W. Dunn. 2022. Characterizing the secret diets of siphonophores (Cnidaria: Hydrozoa) using DNA metabarcoding. PloS One **17**: e0267761. doi:10. 1371/journal.pone.0267761
- Décima, M., M. R. Landry, and B. N. Popp. 2013. Environmental perturbation effects on baseline d 15 N values and zooplankton trophic flexibility in the Southern California Current Ecosystem. Limnol. Oceanogr. **58**: 624–634. doi: 10.4319/lo.2013.58.2.0624
- Décima, M., M. R. Landry, C. J. Bradley, and M. L. Fogel. 2017. Alanine $\delta^{15}N$ trophic fractionation in heterotrophic protists. Limnol. Oceanogr. **62**: 2308–2322. doi:10.1002/lno.10567
- Décima, M., M. R. Stukel, L. López-López, and M. R. Landry. 2019. The unique ecological role of pyrosomes in the Eastern Tropical Pacific. Limnol. Oceanogr. **64**: 728–743. doi: 10.1002/lno.11071
- DeNiro, M. J., and S. Epstein. 1978. Influence of diet on the distribution of carbon isotopes in animals. Geochim. Cosmochim. Acta **42**: 495–506. doi:10.1016/0016-7037(78) 90199-0
- DeNiro, M. J., and S. Epstein. 1981. Influence of diet on the distribution of nitrogen isotopes in animals. Geochim. Cosmochim. Acta **45**: 341–351. doi:10.1016/0016-7037(81) 90244-1
- Doherty, S. C., A. E. Maas, D. K. Steinberg, B. N. Popp, and H. G. Close. 2021. Distinguishing zooplankton fecal pellets as a component of the biological pump using compound-specific isotope analysis of amino acids. Limnol. Oceanogr. **64**: 2827–2841. doi:10.1002/lno.11793
- Fry, B. 2006. Stable isotope ecology. Springer. doi:10.1007/0-387-33745-8
- Germain, L., P. L. Koch, J. T. Harvey, and M. D. McCarthy. 2013. Nitrogen isotope fractionation in amino acids from harbor seals: Implications for compound-specific trophic position calculations. Mar. Ecol. Prog. Ser. **482**: 265–277. doi:10.3354/meps10257
- Gloeckler, K., C. A. Choy, C. C. S. Hannides, H. G. Close, E. Goetze, B. N. Popp, and J. C. Drazen. 2018. Stable isotope analysis of micronekton around Hawaii reveals suspended particles are an important nutritional source in the lower mesopelagic and upper bathypelagic zones. Limnol. Oceanogr. **63**: 1168–1180. doi:10.1002/lno.10762
- Graham, B. S., P. L. Koch, S. D. Newsome, K. W. McMahon, and D. Aurioles. 2010. Using isoscapes to trace the movements and foraging behavior of top predators in oceanic ecosystems, p. 299–318. *In* J. B. West, G. J. Bowen, T. E. Dawson, and K. P. Tu [eds.], Isoscapes. Springer. doi:10. 1007/978-90-481-3354-3_14
- Gutiérrez-Rodríguez, A., M. Décima, B. N. Popp, and M. R. Landry. 2014. Isotopic invisibility of protozoan trophic

- steps in marine food webs. Limnol. Oceanogr. **59**: 1590–1598. doi:10.4319/lo.2014.59.5.1590
- Haddock, S. H., and J. N. Heine. 2005. Scientific blue-water diving. California Sea Grant College Program.
- Haddock, S. H., C. W. Dunn, P. R. Pugh, and C. E. Schnitzler. 2005. Bioluminescent and red-fluorescent lures in a deep-sea siphonophore. Science **309**: 263. doi:10.1126/science. 1110441
- Hannides, C. C. S., B. N. Popp, M. R. Landry, and B. S. Graham. 2009. Quantification of zooplankton trophic position in the North Pacific Subtropical Gyre using stable nitrogen isotopes. Limnol. Oceanogr. **54**: 50–61. doi:10. 4319/lo.2009.54.1.0050
- Hannides, C. C. S., B. N. Popp, C. A. Choy, and J. C. Drazen. 2013. Midwater zooplankton and suspended particle dynamics in the North Pacific Subtropical Gyre: A stable isotope perspective. Limnol. Oceanogr. **58**: 1931–1946. doi: 10.4319/lo.2013.58.6.1931
- Hannides, C. C. S., and others. 2020. Seasonal dynamics of midwater zooplankton and relation to particle cycling in the North Pacific Subtropical Gyre. Prog. Oceanogr. **182**: 102266. doi:10.1016/j.pocean.2020.102266
- Hays, G. C., T. K. Doyle, and J. D. R. Houghton. 2018. A paradigm shift in the trophic importance of jellyfish? Trends Ecol. Evol. **33**: 874–884. doi:10.1016/j.tree.2018.09.001
- Hetherington, E. D., R. J. Olson, J. C. Drazen, C. E. Lennert-Cody, L. T. Ballance, R. S. Kaufmann, and B. N. Popp. 2017. Spatial food-web structure in the eastern tropical Pacific Ocean based on compound-specific nitrogen isotope analysis of amino acids. Limnol. Oceanogr. **62**: 541–560. doi:10. 1002/lno.10443
- Hetherington, E. D., C. A. Choy, E. V. Thuesen, and S. H. D. Haddock. 2022a. Three distinct views of deep pelagic community composition based on complementary sampling approaches. Front. Mar. Sci. **9**: 864004. doi:10.3389/fmars. 2022.864004
- Hetherington, E. D., A. Damian-Serrano, S. H. D. Haddock, C. W. Dunn, and C. A. Choy. 2022*b*. Integrating siphonophores into marine food-web ecology. Limnol. Oceanogr.: Lett. **7**: 81–95. doi:10.1002/lol2.10235
- Hoving, H. J. T., and S. H. D. Haddock. 2017. The giant deepsea octopus *Haliphron atlanticus* forages on gelatinous fauna. Sci. Rep. **7**: 44952. doi:10.1038/srep44952
- Jackson, A. L., R. Inger, A. C. Parnell, and S. Bearhop. 2011. Comparing isotopic niche widths among and within communities: SIBER—Stable Isotope Bayesian Ellipses in R. J. Anim. Ecol. 80: 595–602. doi:10.1111/j.1365-2656.2011. 01806.x
- Kurle, C., and J. K. McWhorter. 2017. Spatial and temporal variability within marine isoscapes: Implications for interpreting stable isotope data from marine systems. Mar. Ecol. Prog. Ser. **568**: 31–45. doi:10.3354/meps12045
- Lam, P. J., and O. Marchal. 2015. Insights into particle cycling from thorium and particle data. Ann. Rev. Mar.

- Sci. **7**: 159–184. doi:10.1146/annurev-marine-010814-015623
- Lam, P. J., S. C. Doney, and J. K. B. Bishop. 2011. The dynamic ocean biological pump: Insights from a global compilation of particulate organic carbon, CaCO₃, and opal concentration profiles from the mesopelagic. Glob. Biogeochem. Cycles **25**: GB3009. doi:10.1029/2010GB003868
- Lamb, P. D., E. Hunter, J. K. Pinnegar, T. K. Doyle, S. Creer, and M. I. Taylor. 2019. Inclusion of jellyfish in 30+ years of Ecopath with Ecosim models. ICES J. Mar. Sci. **76**: 1941–1950. doi:10.1093/icesjms/fsz165
- Landry, M. R., and M. R. Décima. 2017. Protistan microzooplankton and the trophic position of tuna: Quantifying the trophic link between micro- and mesozooplankton in marine foodwebs. ICES J. Mar. Sci. **74**: 1885–1892. doi:10. 1093/icesjms/fsx006
- Lucas, C. H., and others. 2014. Gelatinous zooplankton biomass in the global oceans: Geographic variation and environmental drivers. Glob. Ecol. Biogeogr. **23**: 701–714. doi:10.1111/geb.12169
- Lyle, J. T., R. K. Cowen, S. Sponaugle, and K. R. Sutherland. 2022. Fine-scale vertical distribution and diel migrations of *Pyrosoma atlanticum* in the northern California Current. J. Plankton Res. **44**: 288–302. doi:10.1093/plankt/fbac006
- Mapstone, G. M. 2014. Global diversity and review of Siphonophorae (Cnidaria: Hydrozoa). PloS One **9**: e87737. doi:10.1371/journal.pone.0087737
- McClelland, J. W., and J. P. Montoya. 2002. Trophic relationships and the nitrogen isotopic composition of amino acids in plankton. Ecology **83**: 2173–2180. doi:10.1890/0012-9658(2002)083[2173:TRATNI]2.0.CO;2
- McMahon, K. W., and M. D. McCarthy. 2016. Embracing variability in amino acid $\delta^{15}N$ fractionation: Mechanisms, implications, and applications for trophic ecology. Ecosphere **7**: e01511. doi:10.1002/ecs2.1511
- Milisenda, G., S. Rossi, S. Vizzini, V. L. Fuentes, J. E. Purcell, U. Tilves, and S. Piraino. 2018. Seasonal variability of diet and trophic level of the gelatinous predator *Pelagia noctiluca* (Scyphozoa). Sci. Rep. **8**: 12140. doi:10.1038/s41598-018-30474-x
- Miller, R., H. Page, and M. Brzezinski. 2013. δ13C and δ15N of particulate organic matter in the Santa Barbara Channel: Drivers and implications for trophic inference. Mar. Ecol. Prog. Ser. **474**: 53–66. doi:10.3354/meps10098
- Munro, C., and others. 2018. Improved phylogenetic resolution within Siphonophora (Cnidaria) with implications for trait evolution. Mol. Phylogenet. Evol. **127**: 823–833. doi: 10.1016/j.ympev.2018.06.030
- Pagès, F., and L. P. Madin. 2010. Siphonophores eat fish larger than their stomachs. Deep-Sea Res. II: Top. Stud. Oceanogr. **57**: 2248–2250.
- Parzanini, C., C. C. Parrish, J.-F. Hamel, and A. Mercier. 2017. Trophic ecology of a deep-sea fish assemblage in the

- Northwest Atlantic. Mar. Biol. **164**: 206. doi:10.1007/s00227-017-3236-4
- Patry, W. L., M. Bubel, C. Hansen, and T. Knowles. 2020. Diffusion tubes: A method for the mass culture of ctenophores and other pelagic marine invertebrates. PeerJ **8**: e8938. doi: 10.7717/peerj.8938
- Pauly, D., W. Graham, S. Libralato, L. Morissette, and M. L. D. Palomares. 2009. Jellyfish in ecosystems, online databases, and ecosystem models, p. 67–85. *In* K. A. Pitt and J. E. Purcell [eds.], Jellyfish blooms: Causes, consequences, and recent advances. Springer. doi:10.1007/978-1-4020-9749-2.5
- Popp, B. N., B. S. Graham, R. J. Olson, C. C. Hannides, M. J. Lott, G. A. López-Ibarra, F. Galván-Magaña, and B. Fry. 2007. Insight into the trophic ecology of yellowfin tuna, *Thunnus albacares*, from compound-specific nitrogen isotope analysis of proteinaceous amino acids. Terr. Ecol. 1: 173–190. doi:10.1016/S1936-7961(07)01012-3
- Post, D. M. 2002. Using stable isotopes to estimate trophic position: Models, methods, and assumptions. Ecology **83**: 703–718. doi:10.2307/3071875
- Prairie, J. C., K. Ziervogel, R. Camassa, R. M. McLaughlin, B. L. White, C. Dewald, and C. Arnosti. 2015. Delayed settling of marine snow: Effects of density gradient and particle properties and implications for carbon cycling. Mar. Chem. **175**: 28–38. doi:10.1016/j.marchem.2015.04.006
- Purcell, J. E. 1981*a*. Dietary composition and diel feeding patterns of epipelagic siphonophores. Mar. Biol. **65**: 83–90. doi:10.1007/BF00397071
- Purcell, J. E. 1981*b*. Feeding ecology of *Rhizophysa eysenhardti*, a siphonophore predator of fish larvae. Limnol. Oceanogr. **26**: 424–432. doi:10.4319/lo.1981.26.3.0424
- Rau, G. H., C. Low, J. T. Pennington, K. R. Buck, and F. P. Chavez. 1998. Suspended particulate nitrogen δ15N versus nitrate utilization: Observations in Monterey Bay, CA. Deep Sea Res. Part II Top. Stud. Oceanogr. 45: 1603–1616. doi: 10.1016/s0967-0645(98)80008-8
- Remsen, A., T. L. Hopkins, and S. Samson. 2004. What you see is not what you catch: A comparison of concurrently collected net, optical plankton counter, and shadowed image particle profiling evaluation recorder data from the northeast Gulf of Mexico. Deep-Sea Res. I: Oceangr. Res. Pap. **51**: 129–151. doi:10.1016/j.dsr.2003.09.008
- Richards, T. M., T. T. Sutton, and R. J. D. Wells. 2020. Trophic structure and sources of variation influencing the stable isotope signatures of meso- and bathypelagic micronekton fishes. Front. Mar. Sci. **7**: 507992. doi:10.3389/fmars.2020. 507992
- Robison, B. H., K. R. Reisenbichler, R. E. Sherlock, J. M. B. Silguero, and F. P. Chavez. 1998. Seasonal abundance of the siphonophore, Nanomia bijuga, in Monterey Bay. Deep Sea Res. Part II Top. Stud. Oceanogr. **45**: 1741–1751. doi: 10.1016/s0967-0645(98)80015-5

- Rolff, C. 2000. Seasonal variation in δ^{13} C and δ^{15} N of size-fractionated plankton at a coastal station in the northern Baltic proper. Mar. Ecol. Prog. Ser. **203**: 47–65. doi:10. 3354/meps203047
- Romero-Romero, S., C. A. Ka'apu-Lyons, B. P. Umhau, C. R. Benitez-Nelson, C. C. S. Hannides, H. G. Close, J. C. Drazen, and B. N. Popp. 2020. Deep zooplankton rely on small particles when particle fluxes are low. Limnol. Oceanogr.: Lett. **5**: 410–416. doi:10.1002/lol2.10163
- RStudio Team (2020). RStudio: Integrated development for R. RStudio, Inc. www.rstudio.com/
- Saino, T., and A. Hattori. 1980. 15N natural abundance in oceanic suspended particulate matter. Nature **283**: 752–754. doi:10.1038/283752a0
- Schaub, J., A. K. McLaskey, I. Forster, and B. P. Hunt. 2021. Experimentally derived estimates of turnover and modification for stable isotopes and fatty acids in scyphozoan jellyfish. J. Exp. Mar. Bio. Ecol. **545**: 151631. doi:10.1016/j.jembe.2021.151631
- Schlining, B. M., and N. J. Stout. 2006. MBARI's video annotation and reference system. OCEANS 2006.
- Shea, C. H., P. K. Wojtal, H. G. Close, A. E. Maas, K. Stamieszkin, J. S. Cope, D. K. Steinberg, N. Wallsgrove, and B. N. Popp. 2023. Small particles and heterotrophic protists support the mesopelagic zooplankton food web in the subarctic northeast Pacific Ocean. Limnol. Oceanogr. 68: 1949–1963. doi:10.1002/lno.12397
- Shen, Y., T. P. Guilderson, O. A. Sherwood, C. G. Castro, F. P. Chavez, and M. D. McCarthy. 2021. Amino acid δ^{13} C and δ^{15} N patterns from sediment trap time series and deep-sea corals: Implications for biogeochemical and ecological reconstructions in paleoarchives. Geochim. Cosmochim. Acta **297**: 288–307. doi:10.1016/j.gca.2020.12.012
- White, M. E., P. A. Rafter, B. M. Stephens, M. R. Mazloff, S. D. Wankel, and L. I. Aluwihare. 2022. Stable isotopes of nitrate record effects of the 2015–2016 El Niño and diatom iron limitation on nitrogen cycling in the eastern North Pacific Ocean. Limnol. Oceanogr. **67**: 2140–2156. doi:10. 1002/lno.12194
- Wojtal, P. K., and others. 2023. Deconvolving mechanisms of particle flux attenuation using nitrogen isotopes of amino acids. Limnol. Oceanogr. **68**: 1965–1981. doi:10.1002/lno. 12398
- Yamaguchi, Y. T., and M. D. McCarthy. 2018. Sources and transformation of dissolved and particulate organic nitrogen in the North Pacific Subtropical Gyre indicated by compound-specific δ^{15} N analysis of amino acids. Geochim. Cosmochim. Acta **220**: 329–347. doi:10.1016/j.gca.2017. 07.036
- Zeman, S. M., M. Corrales-Ugalde, R. D. Brodeur, and K. R. Sutherland. 2018. Trophic ecology of the neustonic cnidarian *Velella velella* in the northern California Current during an extensive bloom year: Insights from gut contents and

Trophic ecology of siphonophores

stable isotope analysis. Mar. Biol. **165**: 150. doi:10.1007/s00227-018-3404-1

Acknowledgments

We thank the crews of MBARI's R/V Western Flyer and the remotely operated vehicle Doc Ricketts who assisted with collections of siphonophore specimens on several research cruises. We thank MBARI's Midwater Ecology Team, especially Bruce Robison, who supported the collection of a subset of specimens and analyses on his expeditions. We thank Jared Figurski and Erich Rienecker who assisted with particle sample collection aboard R/V Paragon. Phoebe Lam generously assisted with particle sample collections and provisioned her McLane pumps. This research was supported by the National Science Foundation Awards OCE-1829812 to

C.A. Choy, OCE-1829805 to S.H.D. Haddock, OCE-1829835 to C.W. Dunn, the David and Lucile Packard Foundation, and the RSMAS Student Travel Fund.

Conflict of Interest

This authors declare no conflict of interest.

Submitted 03 January 2023 Revised 07 August 2023 Accepted 02 February 2024

Associate editor: Michael R. Stukel